

In the format provided by the authors and unedited.

Step-defect guided delivery of DNA to a graphene nanopore

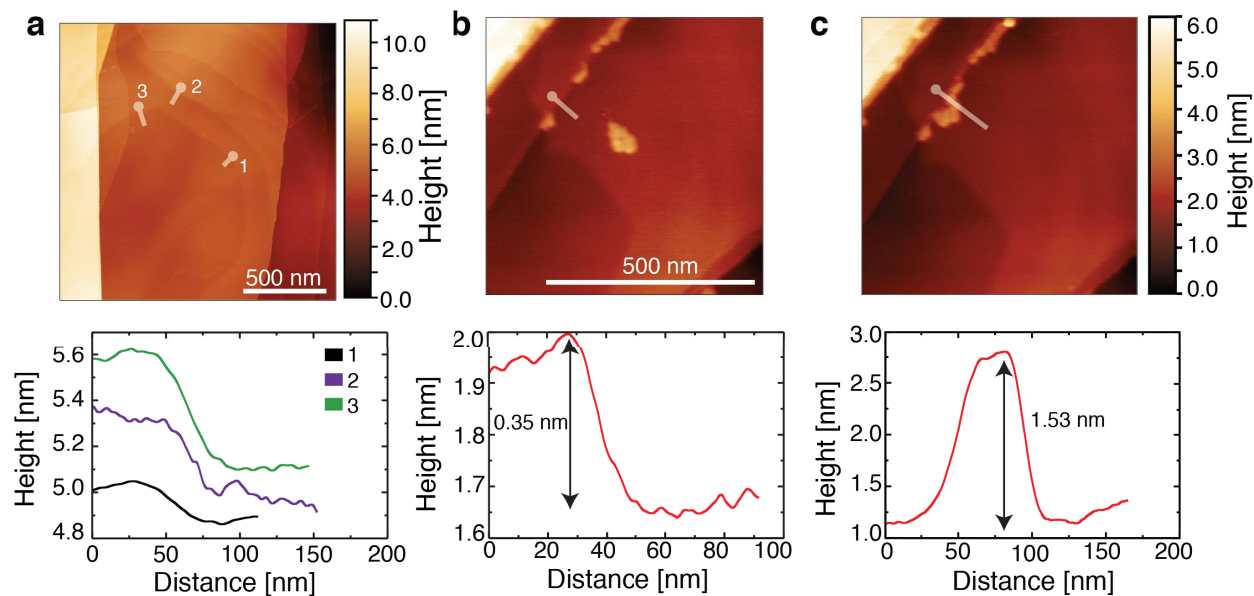
Manish Shankla ¹ and Aleksei Aksimentiev ^{2*}

¹Department of Physics, University of Illinois, Urbana, IL, USA. ²Department of Physics, Beckman Institute for Advanced Science and Technology, University of Illinois, Urbana, IL, USA. *e-mail: aksiment@illinois.edu

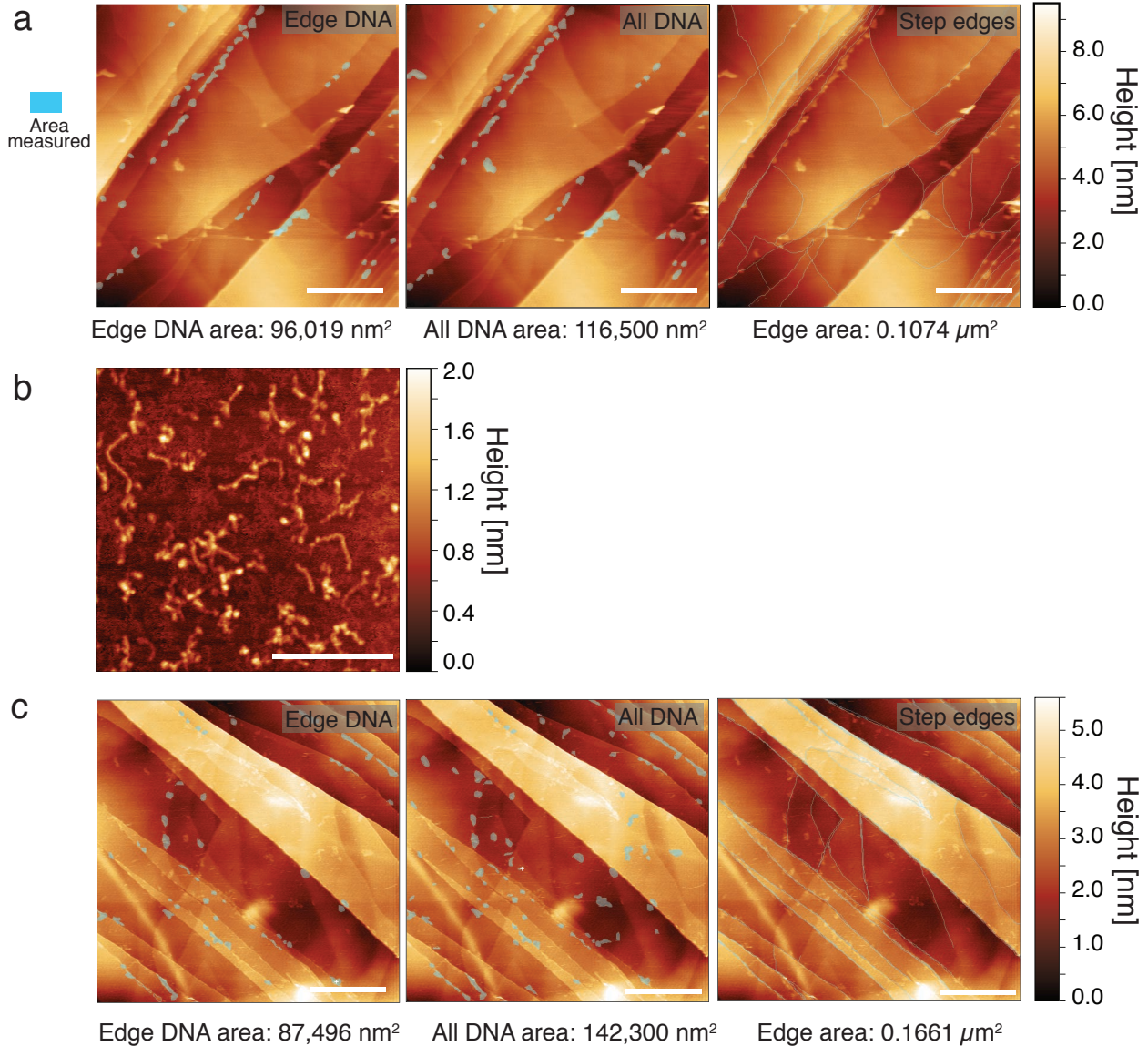
Step-defect guided delivery of DNA to a graphene nanopore

Manish Shankla and Aleksei Aksimentiev

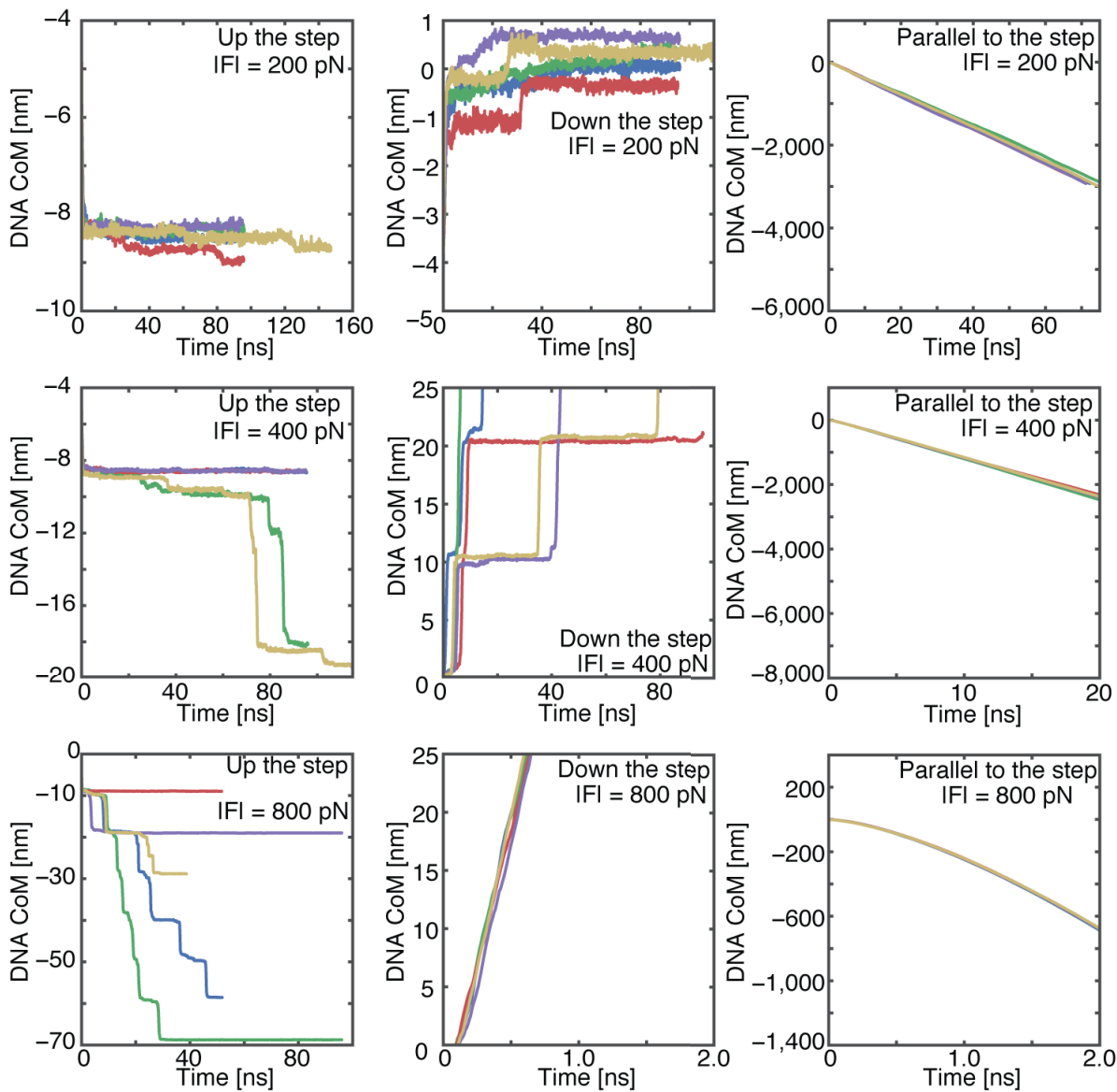
Supplementary Figures	2
Supplementary Fig. 1: AFM images of HOPG	2
Supplementary Fig. 2: Quantitative analysis of DNA coverage of HOPG and mica . . .	3
Supplementary Fig. 3: Simulated displacement of ssDNA subject to constant force . . .	4
Supplementary Fig. 4: SMD simulations of the double layer step defect systems	5
Supplementary Fig. 5: Effect of graphene edge chemistry on directional asymmetry of forced migration	6
Supplementary Fig. 6: Effect of step defect edge geometry on forced migration of ssDNA	7
Supplementary Fig. 7: Illustration of the capture time model	8
Supplementary Fig. 8: Possible approaches to manufacturing guiding structures	9
Supplementary Fig. 9: Possible device-level implementations the guiding structures . .	10
Supplementary Note 1: Rate of nanopore capture in a spiral delivery system	11
Captions to Supplementary Movies	13
Supplementary References	20



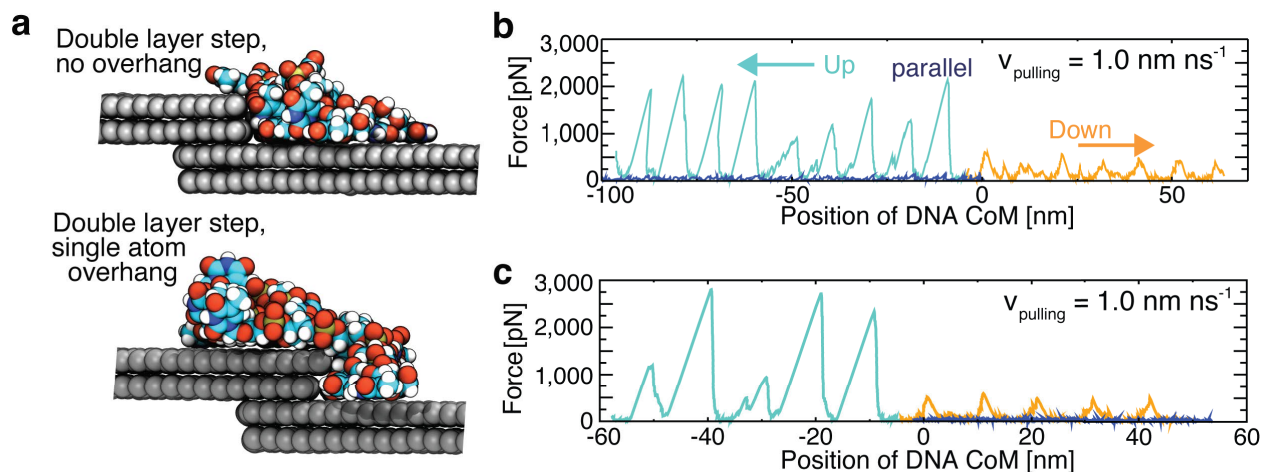
Supplementary Figure 1. AFM images of HOPG. (a) AFM image of a freshly cleaved HOPG surface in air prior to DNA incubation (top). The white lines indicate where the height profiles (shown in the bottom graph) are taken. The circles indicate the starting points (0 nm on the x axis) of the height profiles. (b, c) Two sequential AFM snapshots of an HOPG surface imaged in air after incubation with 0.1 ng/ml of M13 ssDNA. An isolated ssDNA molecule is seen to be displaced by the AFM tip toward a step defect. The height profiles across the step-defect before and after forced migration of the ssDNA molecule are plotted underneath the corresponding snapshots. Supplementary Movies 1 and 2 illustrate the process of ssDNA displacement.



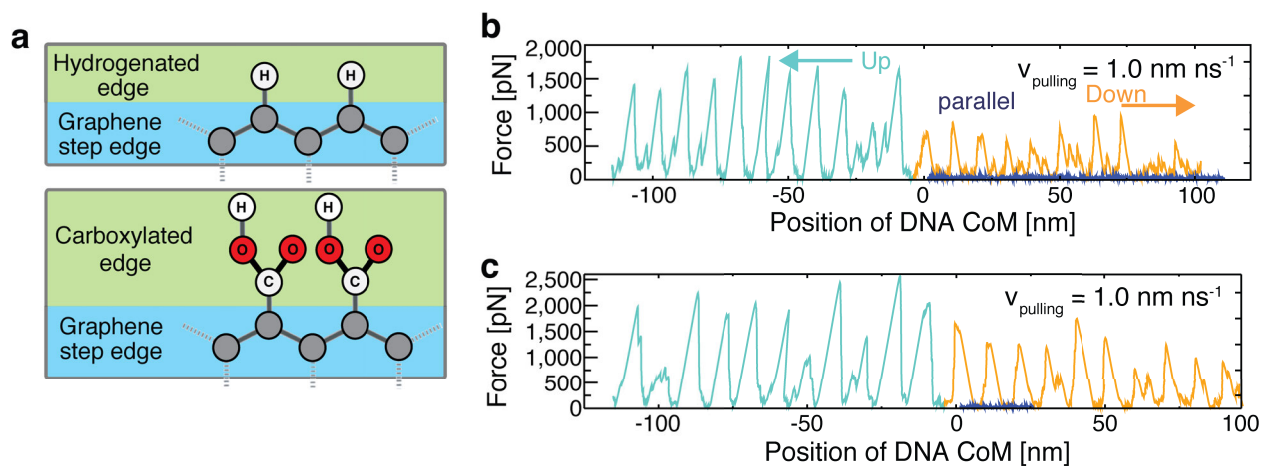
Supplementary Figure 2. AFM images of DNA coverage on HOPG and mica. (a) AFM image of an HOPG sample incubated with 0.1 ng/ml of M13 ssDNA (see Methods) imaged in air. The blue shaded pixels mark the ssDNA molecules located at the step defects (left), ssDNA molecules located anywhere in the image (centre) and just the step edge (right). The location of the DNA molecules and of the step defect edges were identified manually. A small fraction of noisy images of DNA molecules and of step edge fragments were omitted from the analysis. The line identifying the edge was taken to be 2-3 pixels in width; a single pixel has an area of 15.25 nm². The upper bound percentage of the area occupied by the step edge defects was calculated as the ratio of the total area of all edge pixels to the total surface area. The scale bar corresponds to 500 nm. (b) AFM image of a mica sample incubated with 0.1 ng/ml of M13 ssDNA imaged in air. In contrast to ssDNA localisation at the HOPG surface, the DNA molecules on mica appear to be evenly distributed along the surface, which we attribute to the lack of step defects [1]. The scale bar corresponds to 200 nm. (c) Same as in panel a but for an AFM image obtained in solution. The scale bar corresponds to 500 nm. The total area of each image is 4 μm².



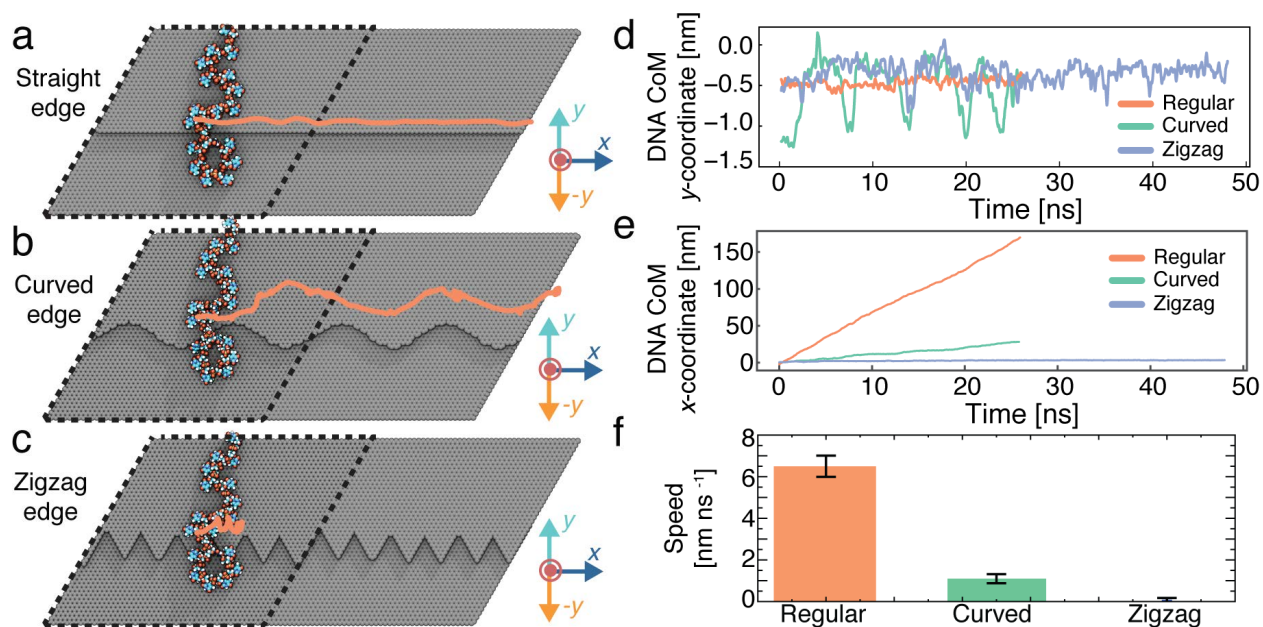
Supplementary Figure 3. Simulated displacement of poly(dT)₂₀ subject to a constant force. The data are organised in columns and rows corresponding to the direction of the constant force (up, down and parallel to the step defect) and the magnitude of the constant force (200, 400 and 800 pN), respectively. In each panel, the DNA's CoM coordinate (y coordinate for up and down force directions and z coordinate for parallel force direction) is plotted versus simulation time. The direction of the constant force (up, down and parallel to the step defect) corresponds to $-y$, $+y$ and $+x$ direction in our coordinate system (defined in main text Fig. 2b). Each trace represents a separate MD simulation.



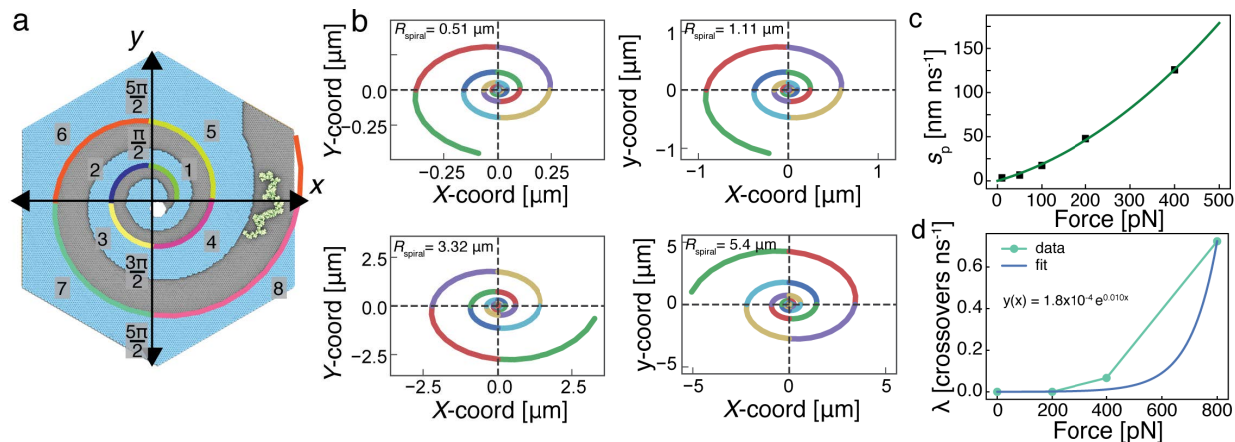
Supplementary Figure 4. The effect of defect height on forced migration of ssDNA. (a) Double layer defects featuring no (top) or a single-atom (bottom) overhang. (b) SMD simulation of poly(dT)₂₀ migration across the double layer defects. The simulation setup is analogous to that shown in the main text Fig. 2a. The SMD force pulling ssDNA is plotted versus the CoM displacement of ssDNA for defects featuring no (top) or a single-atom (bottom) overhang. In each panel, orange, turquoise and blue lines indicate pulling down, up and parallel to the step defect, respectively. In all simulations, the SMD speed was 1.0 nm ns^{-1} .



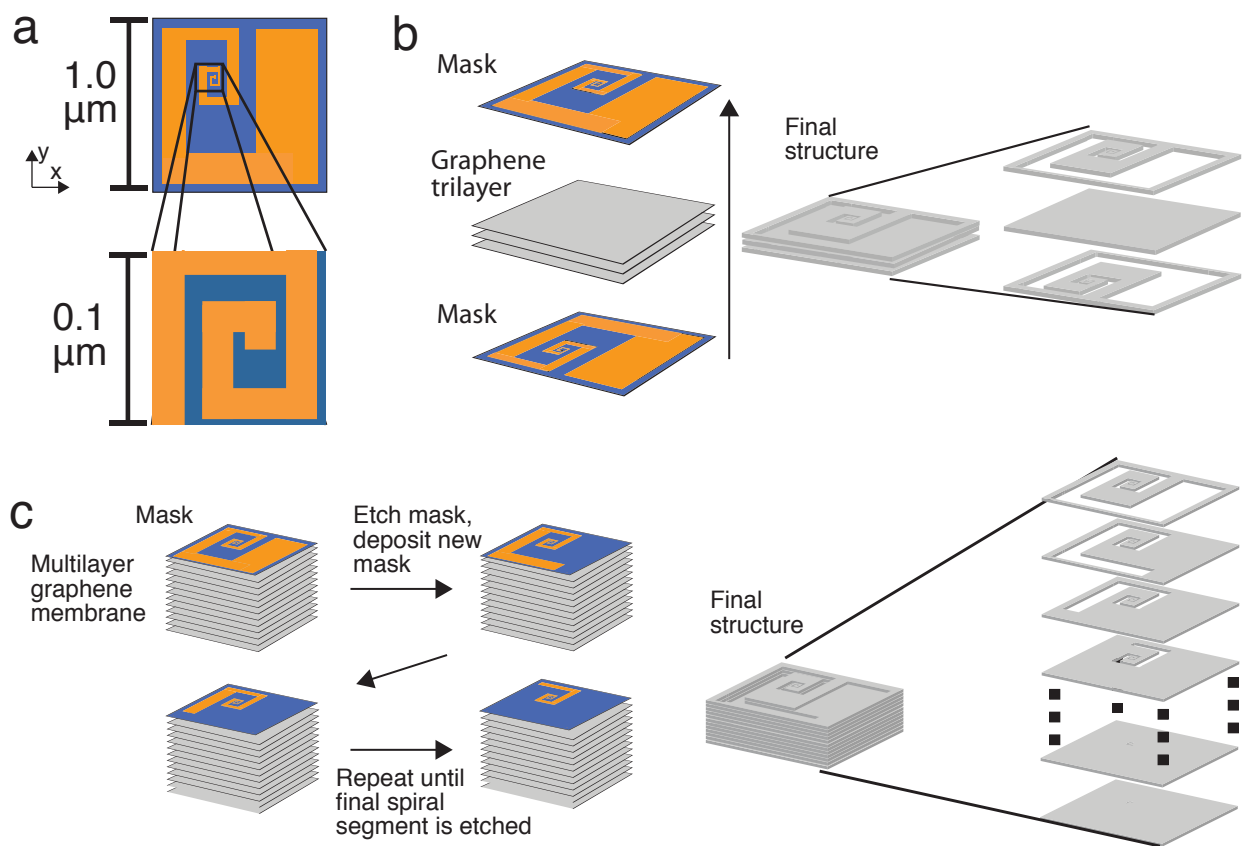
Supplementary Figure 5. The effect of graphene edge termination on forced migration of ssDNA across a step defect. (a) Schematic representation of two types of graphene edge termination: passivation with hydrogen (top) and carboxylation (bottom). (b) SMD simulation of poly(dT)₂₀ migration across the step defect. The simulation setup is analogous to that shown in the main text Fig. 2a. The SMD force pulling ssDNA is plotted versus the CoM displacement of ssDNA for passivated (top) and carboxylated (bottom) step defects. In each panel, orange, turquoise and blue lines indicate pulling down, up and parallel to the step defect, respectively. In all simulations, the SMD speed was 1.0 nm ns^{-1} .



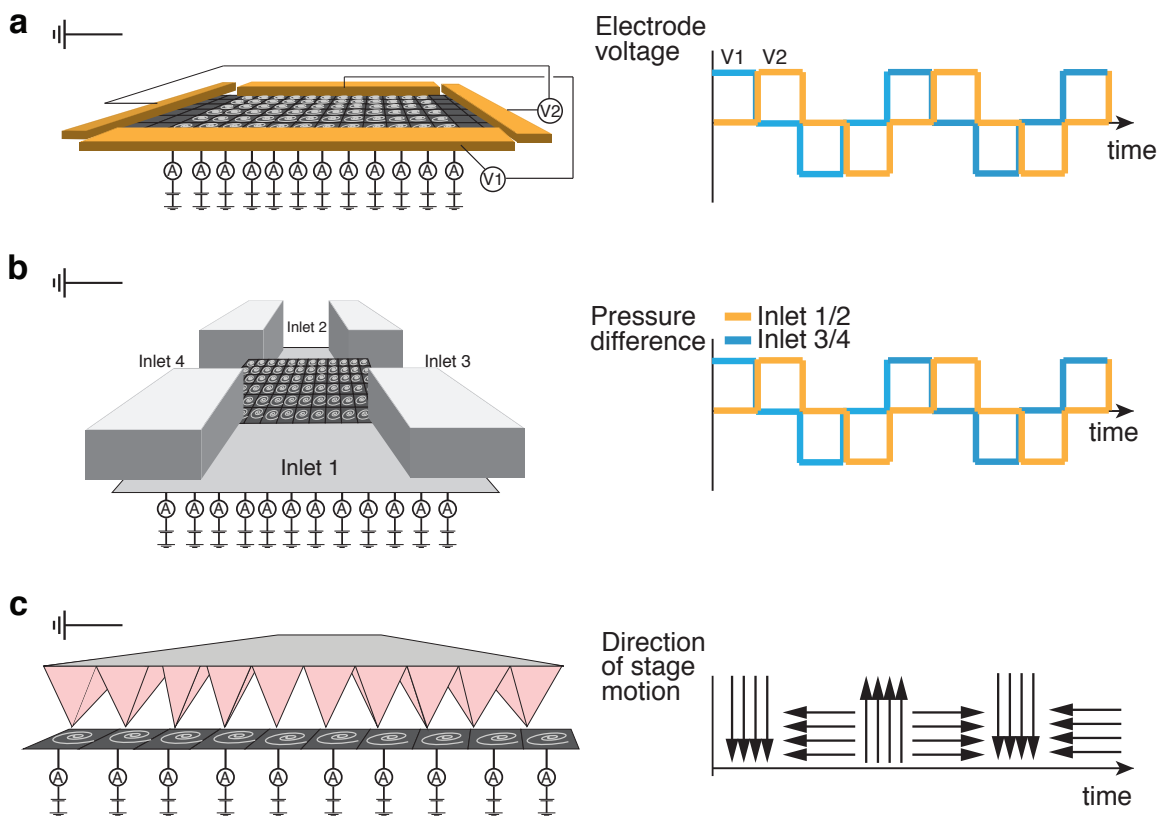
Supplementary Figure 6. The effect of step defect edge geometry on forced migration of ssDNA. (a-c) Initial configuration of poly(dT)₂₀ placed at the edge of a step defect having a straight (a), curved (b) and zigzag (c) geometry. The graphene sheet and ssDNA were submerged in 1M KCl electrolyte (not shown) and equilibrated for 10 ns. Following that, a constant, 50 pN-magnitude force was applied in the $+x$ direction. The orange line illustrates the path of the DNA's CoM during the constant force simulation. (d,e) Y (d) and x (e) CoM coordinates of the DNA molecule during the constant force MD simulation for each step defect geometry. (f) Average speed of the ssDNA molecule in the x direction for each step defect geometry. The average speed was calculated by splitting each MD trajectory into 2.5 ns fragments, finding the average velocity for each fragment and averaging these velocity values. Error bars represent the standard deviation from the mean.



Supplementary Figure 7. Illustration of the capture time model. (a) Overhead view of a parametric curve (multi-coloured line) used for the calculation of the capture time superimposed on the spiral guiding structure used in the all-atom MD simulations, Fig. 6a. Each uniquely coloured segment of the curve spans a polar angle of $\pi/2$. In this figure, the spiral structure consist of eight $\pi/2$ segments. (b) Spiral geometries generated using the same geometric parameters as for the spiral shown in panel a, but for different linear dimensions of the spiral, R_{spiral} . Similar to panel a, each $\pi/2$ segment of the spiral is shown using a different colour. (c) Average speed of ssDNA, s_p pushed by a constant force directed parallel to the step as a function of the force magnitude (black squares) approximated by a least square fit (green line). (d) The rate of ssDNA crossing a step defect, λ , subject to a constant external force directed up the step defect as a function of the force magnitude (green circles). Blue line shows an exponential fit to the data. Data shown in panels b and c are taken from Fig. 4b.



Supplementary Figure 8. Possible approaches to manufacturing right-angled guiding structures. (a) Overhead views of the right-angled guiding structure. The bottom image shows a magnified view of a part of the structure shown in the top image. (b) Schematic of a bottom-up, layer-by-layer fabrication of a guiding structures containing spirals of opposite chirality. Starting from a sacrificial substrate layer (not shown), three graphene layers are grown on top of one another. The spiral structures of opposite chirality are incorporated in layer 1 and 3 of the structure by preventing graphene growth in the regions covered by a mask. The sacrificial substrate and the mask material are etched away, producing a free-standing three-layer graphene structure containing spiral structures of opposite chirality. (c) Schematic of a top-down approach to fabrication of a guiding spiral structure. The structure is produced by repeating the mask deposition and graphene etching steps, removing one graphene layer in each etching step. The mask structures are designed to omit, in each step, the outer most segment of the spiral pattern, ensuring that the depth of the layers increases toward the centre of the spiral. The final structure consists of multiple graphene layers.



Supplementary Figure 9. Possible device-level implementations the guiding structures. An array of nanopores in a thin (e.g. graphene) membrane is placed on top of an array of individually addressable wells made using conventional silicon nanotechnology. Each of the nanopores is surrounded by a guiding structure and exposed to a common solution chamber, where the sample molecules are loaded. The displacement of adhered biomolecules in the sample chamber is produced and directed by either electric field (panel a), a hydrostatic pressure (panel b) or by using a multiplex AFM array (panel c). A set of electrodes is used to impose a voltage difference between the loading chamber and the interior of each well, producing and recording the ionic current individually through each nanopore.

Supplementary Note 1: Rate of nanopore capture in a spiral delivery system

To estimate the average time required to capture an ssDNA molecule by the nanopore located at the centre of a micron-size spiral structure, we assume that an adsorbed ssDNA molecule travels along the outer edge of the spiral, Supplementary Fig. 7a. For the sake of convenience, we assume the spiral structures to have the same shape as in the all-atom MD simulations (see main text Methods for mathematical definition). The arc length of such spiral is $l(\theta) = \frac{a\sqrt{1+b^2}}{b}e^{b\theta}$, where θ is a parametric variable—the polar angle, and $a = 30 \text{ \AA}$ and $b = 0.14$ are the geometric parameters defining the shape of the spiral. The spiral structures considered in our theoretical analysis have θ values in the range from 0 to 28π , which corresponds to the spiral outer radii, R_{spiral} , ranging from 0 to 5.4 \mu m , with $\theta = 0$ being the location of the nanopore. Supplementary Fig. 7b illustrates several representative spiral structures having different R_{spiral} values.

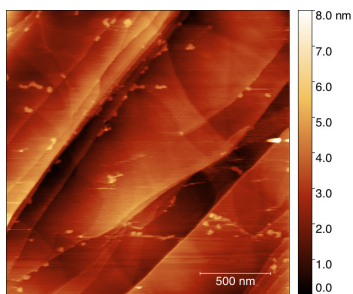
In our nanopore capture protocol, an external guiding force of magnitude f changes its direction clockwise every time interval τ . Our all-atom MD simulation (Fig. 6b and Supplementary Movies 11–13) show that, subject to a constant external force, a molecule of ssDNA adsorbed to a spiral-shaped step defect travels along the step defect. The average arc length that the molecule travels can be approximated as $s_p(f)/\tau$, where s_p is the speed of the adsorbed molecule subject to a constant external force of magnitude f . For ssDNA, we determine s_p by extrapolation of the data obtained from all-atom MD simulations of ssDNA displacement parallel to the step defect, Supplementary Fig. 7c. The adsorbed molecule can be captured by the guiding structure if the arc length of any of its $n \pi/2$ fragments, $\Delta l(n) = l(n\pi/2) - l(n\pi/2 - \pi/2)$, is less than $s_p(f)/\tau$. In that case, the total time required to capture the molecule is $n \times \tau$. If the arc length of any of the $\pi/2$ fragments of the spiral is greater than $s_p(f)/\tau$, the guiding force protocol will not produce nanopore capture. Thus, for a fixed size of the spiral structure and a fixed duration of the constant force application, the magnitude of the guiding force must exceed a threshold value to produce nanopore capture.

On the other hand, the guiding force should be small enough not to push the adsorbed molecule over the step defect. In our MD simulation, Supplementary Movies 11-13, we observed the ssDNA molecule to be pushed directly against the spiral edge after traversing a $\pi/2$ segment. We can estimate the duration of time the ssDNA molecule is pushed against the spiral edge as the difference

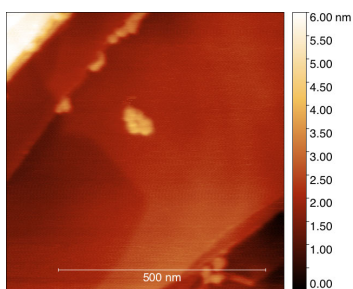
between the duration of the constant force application and the time it takes for the ssDNA molecule to traverse the segment: $\Delta t(f, n) = \tau - \frac{\Delta l(n)}{s_p(f)}$. For a spiral segment, n , we model the probability of the step defect crossing as Poisson process, $P_{\text{cross}}(\Delta t(f, n)) = 1 - e^{-\lambda(f)\Delta t(f, n)}$, where $\lambda(f)$ is the force magnitude-dependent frequency of ssDNA crossing a step defect. We estimate $\lambda(f)$ using an exponential fit to the all-atom MD data, Supplementary Fig. 7d, where the simulated $\lambda(f)$ values were obtained by dividing the average speed of ssDNA up the step defect (main text Fig. 4b) by the distance between two consecutive detects in the MD simulation system, 11.4 nm.

For the force magnitude, f , and duration, τ , in the 0.5–5.0 pN and 2–25 μs range, the probability of defect skipping, P_{cross} is close to zero and the nanopore capture time is well approximated by $T_{\text{capture}}(n, \tau) = n \times \tau$, where n is the number of $\pi/2$ segments of the logarithmic spiral of the outer radius R_{spiral} , i.e., $n = 2/(\pi b) \ln(R_{\text{spiral}}/a)$. This approximation was directly verified by stochastic simulations of nanopore capture. The maximum theoretical throughput of an array of nanopores is then $p/T_{\text{capture}}(n, \tau)$, where p is the number of nanopores per unit area. Thus, according to Fig. 6f of the main text, a device featuring one spiral structure per 1 μm^2 would have a maximum theoretical throughput of 10^2 molecules per second per μm^2 at a 0.5 pN magnitude of the applied force and a 360 μs cycle time, assuming DNA capture is the rate limiting step of the sequencing process.

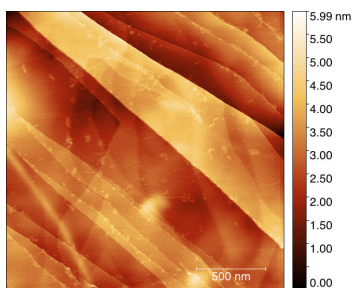
For comparison, we estimate the throughput of the minIon device considering that each device processes 20 Gb per 48 hours and the read length of one molecule is approximately 5 kB as reported by Oxford Nanopore technologies [2]. Hence, we took 20 gB/48 hours \times (1 molecule / 5kB) = 23.1 molecules/sec/device as an approximate throughput. The device sensing area was estimated from a visual depiction of the nanopore cell [3] and calculated to be 26 mm^2 . The minIon’s throughput was then estimated as 9×10^{-7} molecules per second per μm^2 , which is many order of magnitude less than the maximum theoretical throughput of a nanopore array decorated by our guiding structures. While the above calculations provide, at best, an order of magnitude estimate, they nevertheless clearly show a dramatic speed up that a deterministic delivery of DNA to a nanopore array can offer in comparison to a reliance on stochastic nanopore capture.



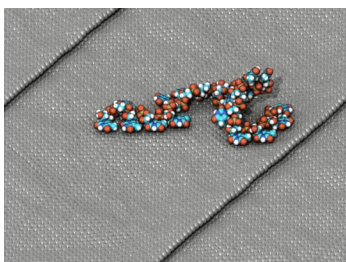
Supplementary Movie 1. Displacement of M13 ssDNA on freshly cleaved HOPG imaged in air using AFM. Prior to imaging, the HOPG sample was incubated with 0.1 ng/ml of M13 ssDNA. Still images from this animation are shown in Supplementary Fig. 1.



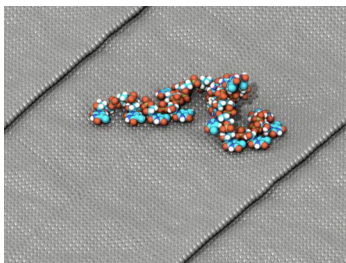
Supplementary Movie 2. Zoomed-in view on ssDNA aggregation and displacement. The sequence of images is the same as in Supplementary Movie 1.



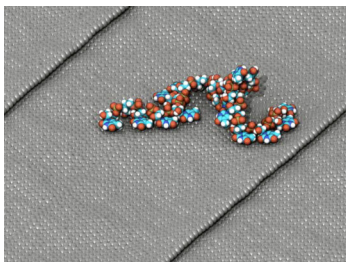
Supplementary Movie 3. Displacement of M13 ssDNA on freshly cleaved HOPG imaged in solution using AFM. Prior to imaging, the HOPG sample was incubated with 0.1 ng/ml of M13 ssDNA. Still images from this movie are shown in Fig. 1c of the main text and analysed quantitatively in Supplementary Figure 2.



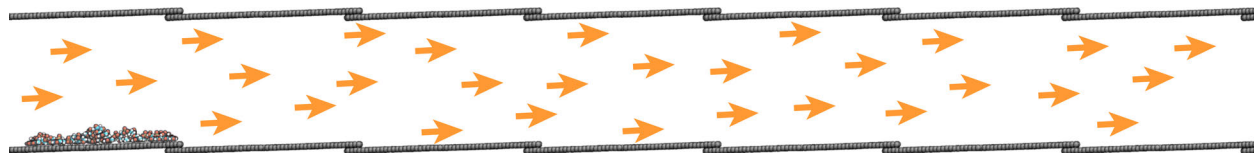
Supplementary Movie 4. Forced migration of poly(dT)₂₀ down a step defect on a graphene membrane (grey). The CoM of the ssDNA molecule is attached to a spring and pulled with a constant velocity of 1.0 nm ns⁻¹. The DNA molecule is shown using van der Waals (vdW) spheres colored according to the atom type: blue (nitrogen), red (oxygen), white (hydrogen), carbon (cyan) and gold (phosphorous). The movie illustrates a 25 ns fragment of an MD trajectory.



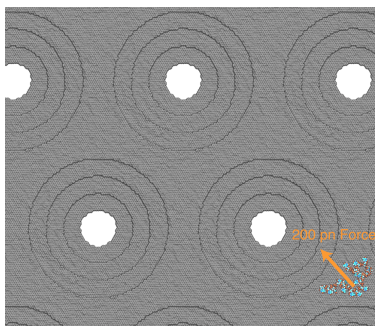
Supplementary Movie 5. Forced migration of poly(dT)₂₀ up a step defect on a graphene membrane (grey). The CoM of the ssDNA molecule is attached to a spring and pulled with a constant velocity of 1.0 nm ns⁻¹. The DNA molecule is shown using vdW spheres colored according to the atom type: blue (nitrogen), red (oxygen), white (hydrogen), carbon (cyan) and gold (phosphorous). The movie illustrates a 25 ns fragment of an MD trajectory.



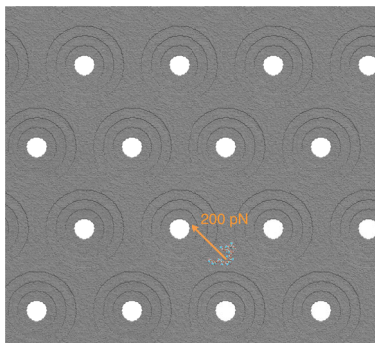
Supplementary Movie 6. Forced migration of poly(dT)₂₀ parallel to a step defect on a graphene membrane (grey). The CoM of the ssDNA molecule is attached to a spring and pulled with a constant velocity of 1.0 nm ns⁻¹. The DNA molecule is shown using vdW spheres colored according to the atom type: blue (nitrogen), red (oxygen), white (hydrogen), carbon (cyan) and gold (phosphorous). The movie illustrates a 20 ns fragment of an MD trajectory.



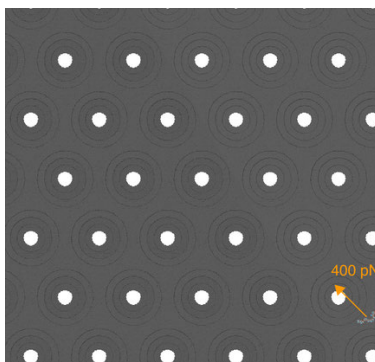
Supplementary Movie 7. Directional displacement of a poly(dT)₂₀ strand along a graphene membrane (grey) driven by water flow that periodically reverses direction. Multiple images of the unit cell are shown for clarity. The flow was produced by the application of a ± 9.2 bar nm⁻¹ pressure gradient. The direction of the flow alternates between pointing down (orange arrows) and up (cyan arrows) the step defect. The DNA is shown using vdW spheres colored according to the atom type: blue (nitrogen), red (oxygen), white (hydrogen), carbon (cyan) and gold (phosphorous). The movie illustrates a 110 ns MD trajectory.



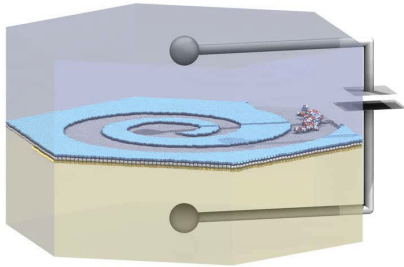
Supplementary Movie 8. Force migration of poly(dT)₂₀ along a nanopore array in a four-layer graphene membrane (grey). Each nanopore is surrounded by three concentric single-atom step defects. The direction of the 200 pN-magnitude force reverses every 3 ns. A 500 mV transmembrane bias is applied throughout the simulation. The DNA is shown using vdW spheres colored according to the atom type: blue (nitrogen), red (oxygen), white (hydrogen), carbon (cyan) and gold (phosphorous). The movie illustrates a 21 ns MD trajectory.



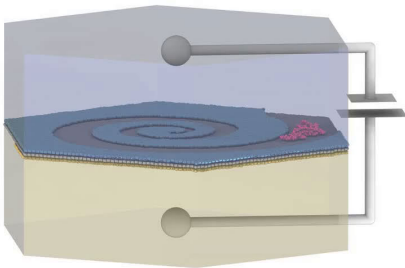
Supplementary Movie 9. Force migration of poly(dT)₂₀ along a nanopore array in a four-layer graphene membrane (grey). Each nanopore is surrounded by three concentric single-atom step defects. The direction of the 200 pN-magnitude force reverses every 10 ns. A 500 mV transmembrane bias is applied throughout the simulation. The DNA is shown using vdW spheres colored according to the atom type: blue (nitrogen), red (oxygen), white (hydrogen), carbon (cyan) and gold (phosphorous). The movie illustrates a 50 ns MD trajectory.



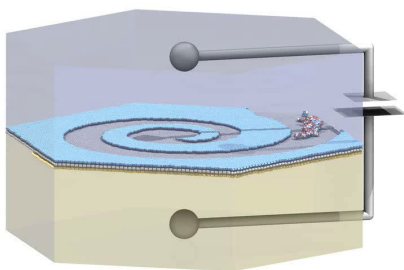
Supplementary Movie 10. Force migration of poly(dT)₂₀ along a nanopore array in a four-layer graphene membrane (grey). Each nanopore is surrounded by three concentric single-atom step defects. The direction of the 400 pN-magnitude force reverses every 10 ns. A 500 mV transmembrane bias is applied throughout the simulation. The DNA is shown using vdW spheres colored according to the atom type: blue (nitrogen), red (oxygen), white (hydrogen), carbon (cyan) and gold (phosphorous). The movie illustrates a 50 ns MD trajectory.



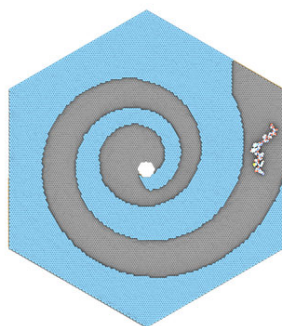
Supplementary Movie 11. Guided transport of poly(dT)₂₀ to and from a nanopore at the center of the spiral structure. The graphene nanostructure consists of a three-layer graphene membrane that has an atom-depth spiral pattern cutout in the outer two layers (yellow, blue). An external force of a 300 pN magnitude is applied to the DNA molecule. The direction of the force changes by 90 degrees clockwise every 5 ns for a total of 26 constant force fragments. A transmembrane potential of 500 mV is applied throughout the simulation. The DNA is shown using vdW spheres colored according to the atom type: blue (nitrogen), red (oxygen), white (hydrogen), carbon (cyan) and gold (phosphorous). The movie illustrates a 130 ns MD trajectory.



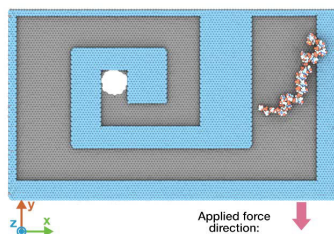
Supplementary Movie 12. Guided transport of poly(dT)₂₀ to and from a nanopore at the center of the spiral structure. The graphene nanostructure consists of a three-layer graphene membrane that has an atom-depth spiral pattern cutout in the outer two layers (yellow, blue). An external force of a 200 pN magnitude is applied to the DNA molecule. The direction of the force changes by 90 degrees clockwise every 7.5 ns for the first five constant force fragments and every 15 ns for the rest of the simulation. One accidental force reversal occurred at step 6. A transmembrane potential of 500 mV is applied throughout the simulation. The DNA is shown using vdW spheres colored red. The movie illustrates a 328 ns MD trajectory.



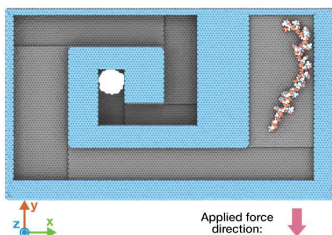
Supplementary Movie 13. Guided transport of poly(dT)₂₀ to and from a nanopore at the center of the spiral structure driven by a flow of solvent. The graphene nanostructure consists of a three-layer graphene membrane that has an atom-depth spiral pattern cutout in the outer two layers (yellow, blue). A solvent flow is produced by a pressure gradient of 3.0 bar nm^{-1} . The direction of the force changes by 90 degrees clockwise every 5 ns. A transmembrane potential of 500 mV is applied throughout the simulation. The DNA is shown using vdW spheres colored according to the atom type: blue (nitrogen), red (oxygen), white (hydrogen), carbon (cyan) and gold (phosphorous). The movie illustrates a 234 ns MD trajectory.



Supplementary Movie 14. Guided transport of a twenty-residue fragment of the α -hemolysin protein (residues 110 to 130) to the nanopore at the center of the spiral structure. The graphene nanostructure consists of a three-layer graphene membrane that has an atom-depth spiral pattern cutout in the outer two layers (yellow, blue). An external force of a 300 pN magnitude is applied to the protein fragment. The direction of the force changes by 90 degrees clockwise every 7.5 ns. The protein is shown using vdW spheres colored according to the atom type: blue (nitrogen), red (oxygen), white (hydrogen), carbon (cyan) and yellow (sulphur). The movie illustrates a 234 ns MD trajectory.



Supplementary Movie 15. Guided transport of poly(dT)₂₀ to a nanopore at the center of a right-angled spiral structure. The graphene nanostructure consists of a two-layer graphene membrane that has an atom-depth right-angled spiral pattern cut in the top layer (blue). An external force of a 300 pN magnitude is applied to the DNA molecule. The direction of the force (indicated by the arrow in the animation) changes by 90 degrees clockwise every 5 ns. The DNA is shown using vdW spheres colored according to the atom type: blue (nitrogen), red (oxygen), white (hydrogen), carbon (cyan) and gold (phosphorous). The movie illustrates a 50 ns MD trajectory.



Supplementary Movie 16. Guided transport of poly(dT)₂₀ to a nanopore at the center of a right-angled spiral structure of increasing depth. The graphene nanostructure consists of eight graphene layers. Each layer contains a segment of a rectangular spiral, starting from the outermost segment. The spiral pattern increases in depth by a single atomic layer with each right-angle turn. An external force of a 300 pN magnitude is applied to the DNA molecule. The direction of the force (indicated by the arrow in the animation) changes by 90 degrees clockwise every 7 ns. The DNA is shown using vdW spheres colored according to the atom type: blue (nitrogen), red (oxygen), white (hydrogen), carbon (cyan) and gold (phosphorous). The movie illustrates a 154 ns MD trajectory.

References

- [1] Rivetti, C., Guthold, M. & Bustamante, C. Scanning force microscopy of dna deposited onto mica: Equilibration versus kinetic trapping studied by statistical polymer chain analysis. *J. Mol. Biol. Evol.* **264**, 919–932 (1996).
- [2] Oxford Nanopore Technology. Minion (2019). URL <https://nanoporetech.com/products/minion>.
- [3] Ward, A. C. & Kim, W. Minion: New, long read, portable nucleic acid sequencing device. *J. Bacteriol. Virol.* **45**, 285–303 (2015).